



UNIVERSITY OF LEEDS

This is a repository copy of *Large scale optimization of transonic axial compressor rotor blades*.

White Rose Research Online URL for this paper:

<https://eprints.whiterose.ac.uk/4765/>

---

**Proceedings Paper:**

Shahpar, S., Polynkin, A. and Toropov, V. (2008) Large scale optimization of transonic axial compressor rotor blades. In: 49th AIAA/ASME/ASCE/AHS/ASC Structures, Structural Dynamics, and Materials Conference. Structures, Structural Dynamics and Materials Conference, 07-10 Apr 2008, Schaumburg, Illinois, USA. Conference Proceeding Series . AIAA .

<https://doi.org/10.2514/6.2008-2056>

---

**Reuse**

Items deposited in White Rose Research Online are protected by copyright, with all rights reserved unless indicated otherwise. They may be downloaded and/or printed for private study, or other acts as permitted by national copyright laws. The publisher or other rights holders may allow further reproduction and re-use of the full text version. This is indicated by the licence information on the White Rose Research Online record for the item.

**Takedown**

If you consider content in White Rose Research Online to be in breach of UK law, please notify us by emailing [eprints@whiterose.ac.uk](mailto:eprints@whiterose.ac.uk) including the URL of the record and the reason for the withdrawal request.



[eprints@whiterose.ac.uk](mailto:eprints@whiterose.ac.uk)  
<https://eprints.whiterose.ac.uk/>

# Large Scale Optimization of Transonic Axial Compressor Rotor Blades

Shahrokh Shahpar\*

*Rolls-Royce plc, Derby, DE24 8BJ, UK*

Andrey Polynkin†, Vassili Toropov‡

*University of Leeds, Leeds, LS2 9JT, UK*

## I. Problem Formulation

In the present work the Multipoint Approximation Method (MAM) by Toropov et al. (1993) has been applied to the shape optimization of an existing transonic compressor rotor (NASA rotor 37) as a benchmark case. Simulations were performed using the Rolls-Royce plc. PADRAM-HYDRA system (Shahpar and Lapworth 2003, Lapworth and Shahpar 2004) that includes the parameterization of the blade shape, meshing, CFD analysis, post-processing, and objective/constraints evaluation. The parameterization approach adopted in this system is very flexible but can result in a large scale optimization problem.

For this pilot study, a relatively coarse mesh has been used including around 470,000 nodes. The parameterization was done using 5 engineering blade parameters like axial movement of sections along the engine axis in mm (XCEN), circumferential movements of sections in degrees (DELTA), solid body rotation of sections in degrees (SKEW), and leading/trailing edge recambering (LEM0/TEM0) in degrees. The design variables were specified using 6 control points at 0 % (hub), 20%, 40%, 60%, 80%, and 100% (tip) along the span. Thus the total number of independent design variables  $N$  was 30. B-spline interpolation was used through the control points to generate smooth design perturbations in the radial direction.

The objective function is the adiabatic efficiency that has to be maximized

$$\eta = \frac{(P_{outlet} / P_{inlet})^{(\gamma-1)/\gamma} - 1}{T_{outlet} / T_{inlet} - 1}$$

where  $P$  and  $T$  are total mass averaged pressure and temperature, respectively. The constraints are the pressure ratio and mass flow rate that have to be within 1% of the same characteristic for the datum blade, i.e.  $2.15 \pm 1.0\%$  for pressure ratio and  $20.1 \text{ kg/s} \pm 0.5\%$  for mass flow rate.

## II. Software Tools

In this work the Rolls-Royce SOFT-PADRAM-HYDRA design system (SOPHY) is used. SOPHY (Shahpar 2004) is a fully integrated flexible aerodynamic design optimization system. The main elements of the SOPHY system are as follows:

SOFT provides four state-of-the-art optimization libraries namely, local and global optimization algorithms, Design of Experiment (DoE), Statistical Variational Analysis (ANOVA) and Response Surface Methodology (RSM). SOFT also provides an integrating platform to define the automation strategy, see Figure 1.

PADRAM is a multi-passage, multi-stage parametric geometry modeller and rapid meshing system. The PADRAM design space for the blades consists of global parameters such as stagger angle, camber angles at leading and trailing edges, lean and sweep at different spanwise locations and pitch (rotor and stator). The PADRAM design space has recently been extended to include an endwall profiling and fillet design capability. PADRAM uses an automatic multiblock mesh generator to create the grid consisting of O-H-C topology. The mesh generation is very fast and does not require user interaction during the optimization. The parametric design system has been extended to non-blading applications, for example nacelle design and exhaust design systems (Lapworth and Shahpar 2004).

---

\* RR Engineering Associate Fellow - Aerothermal Design Systems, AIAA Associate Fellow, FRAeS

† Research Fellow

‡ Professor of Aerospace and Structural Engineering, AIAA Associate Fellow

HYDRA provides a linear and non-linear, parallel multistage Navier-Stokes steady/unsteady state, unstructured solver with the Spalart-Allmaras and K- $\epsilon$  turbulence models. Hydra also provides an Adjoint capability which has recently been demonstrated as part of the SOPHY system. Both mixing and sliding plane can be used to define the interface between the rotating and the stationary blade rows. The HYDRA parallel version allows for splitting a multi-stage analysis into several CPUs (one row per processor or by using a general domain decomposition), hence allowing for faster design evaluations.

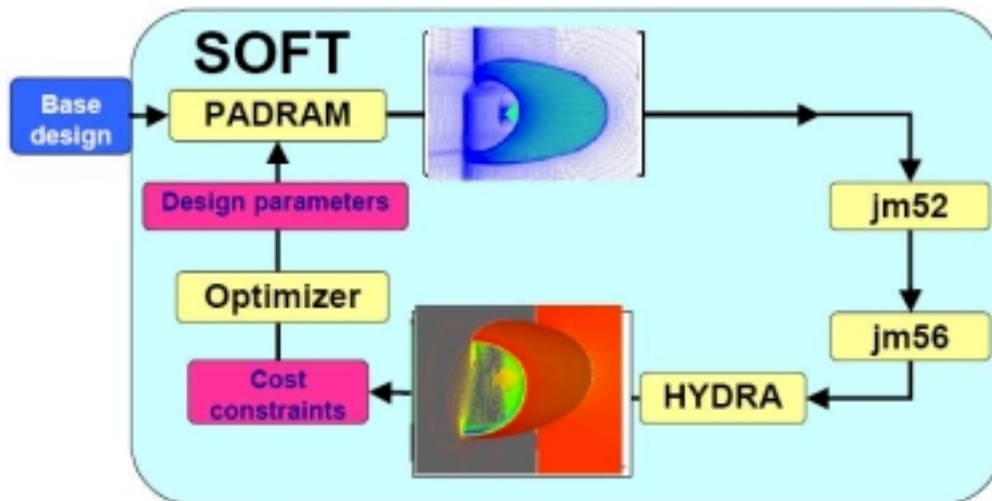


Figure 1: Flowchart of the SOPHY Optimization System

### III. Multipoint Approximation Method (MAM)

This technique (Toropov et al., 1993) replaces the original optimization problem by a succession of simpler mathematical programming problems. The functions in each iteration present mid-range approximations to the corresponding original functions. These functions are noise-free. The solution of an individual sub-problem becomes the starting point for the next step, the move limits are changed and the optimization is repeated iteratively until the optimum is reached. Each approximation function is defined as a function of design variables as well as a number of tuning parameters. The latter are determined by the weighted least squares surface fitting using the original function values (and their derivatives, when available) at several points of the design variable space. This selection of points will be referred to as a plan (design) of numerical experiments. Some of the plan points are generated in a current iteration, and the rest is taken from the pool of points considered in the previous iterations.

A general optimization problem can be formulated as

$$F_0(\mathbf{x}) \rightarrow \min, \quad F_j(\mathbf{x}) \leq 1 \quad (j = 1, \dots, M), \quad A_i \leq x_i \leq B_i \quad (i = 1, \dots, N) \quad (1)$$

where  $\mathbf{x}$  refers to the vector of design variables. In order to reduce the number of calls for the response function evaluations and to lessen the influence of noise, the MAM replaces the optimization problem by a sequence of approximate optimization problems:

$$\tilde{F}_0^k(\mathbf{x}) \rightarrow \min, \quad \tilde{F}_j^k(\mathbf{x}) \leq 1 \quad (j = 1, \dots, M), \quad A_i^k \leq x_i \leq B_i^k, \quad A_i^k \geq A_i, \quad B_i^k \leq B_i \quad (i = 1, \dots, N) \quad (2)$$

where  $k$  is the iteration number.

The selection of the noise-free approximate response functions  $\tilde{F}_j^k(\mathbf{x})$  ( $j = 0, \dots, M$ ) is such that their evaluation is inexpensive as compared to the evaluation of the response functions  $F_j$ , although they are not necessarily explicit functions of the design variables. The approximate response functions are intended to be adequate in a current search sub-domain. This is achieved by appropriate planning of numerical experiments and use of move limits defined by the side constraints  $A_i^k$  and  $B_i^k$ . Moreover, it is attempted to achieve the best quality of the

approximation functions in those regions of the design variable space where the solution of the approximate optimization problem can be expected, e.g. on the boundary of the feasible region.

The approximations are determined by means of weighted least squares:

$$G_j(\mathbf{a}_j) = \sum_{p=1}^P w_{pj} [F_j(\mathbf{x}_p) - \tilde{F}_j(\mathbf{x}_p, \mathbf{a}_j)]^2 \rightarrow \min \quad (3)$$

Here minimization is carried out with respect to the tuning parameters  $\mathbf{a}_j$  and  $w_{pj}$  refers to the weight coefficients. Their selection will be discussed in a subsequent section.

If the first order derivatives  $F_{j,i}(\mathbf{x}) = \partial F_j(\mathbf{x}) / \partial x_i$  at plant points  $\mathbf{x}_p$  are known, the least-squares surface fitting is equivalent to the minimization of the function

$$G_j(\mathbf{a}_j) = \sum_{p=1}^P w_{pj} \left\{ [F_j(\mathbf{x}_p) - \tilde{F}_j(\mathbf{x}_p, \mathbf{a}_j)]^2 + \gamma \delta_{pj} \sum_{i=1}^N [F_{j,i}(\mathbf{x}_p) - \tilde{F}_{j,i}(\mathbf{x}_p, \mathbf{a}_j)]^2 \right\} \rightarrow \min \quad (4)$$

where  $\delta_{pj} = 1 / \sum_{i=1}^N [F_{j,i}(\mathbf{x}_p)]^2$  is a normalizing coefficient and  $0 < \gamma < 1$  reflects the weight of the information on the sensitivities as compared to the information on the function values.

### Intrinsically Linear Approximations

To construct the simplified expressions  $\tilde{F}_j^k(\mathbf{x})$ , it is necessary to define them as a function of tuning parameters  $\mathbf{a}$ . The approximate response functions must be flexible enough to mimic the behaviour of the response functions with sufficient accuracy. On the other hand, they must be easy to evaluate and should not possess any significant level of numerical noise. To simplify notation, we will suppress the indices on the functions  $F_j(\mathbf{x})$  and  $\tilde{F}_j^k(\mathbf{x})$ . The simplest case is a linear function of the tuning parameters  $\mathbf{a}$ :

$$\tilde{F}(\mathbf{x}) = a_0 + \sum_{l=1}^L \varphi_l(\mathbf{x}) a_l \quad (5)$$

Note that the structure of the simplified expression (5) is rather general because the individual regressors  $\varphi_l$  can be arbitrary functions of design variables.

The procedure described above can be further generalized by the application of *intrinsically linear* functions (Draper and Smith, 1981). Such functions are nonlinear, but they can be led to linear ones by simple transformations. The most useful function among them is the multiplicative function

$$\tilde{F}(\mathbf{x}) = a_0 \prod_{l=1}^L \varphi_l(\mathbf{x})^{a_l} \quad (6)$$

with the logarithmic transformation  $\ln \tilde{F}(\mathbf{x}) = \ln a_0 + \sum_{l=1}^L a_l \ln \varphi_l(\mathbf{x})$ .

Intrinsically linear functions have been successfully used for a variety of design optimization problems. The advantage of these approximation functions is that a relatively small number of tuning parameters  $a_i$  is to be determined, and the corresponding least squares problem is solved easily. This is the most important feature of such approximations as it allows to apply them to large scale optimization problems.

## Rational Approximations

An approach is being investigated in the attempt to produce new high quality approximations valid for a larger range of design variables that is based on the use of rational approximations that are a particular class of functions nonlinear in unknown coefficients. This type of approximations was studied before by, e.g. Burgee et al. (1994) and Salazar Celis et al. (2007).

Due to rapidly growing number of coefficients for large  $N$  (that is the main objective of this work), the function structure has to be limited to low degree polynomials (e.g. linear) and small datasets:

$$F(\mathbf{x}) = \frac{a_1 + a_2 x_1 + a_3 x_2 + \dots + a_{n+1} x_n}{1 + a_{n+2} x_1 + a_{n+3} x_2 + \dots + a_{2n+1} x_n} \quad (7)$$

The behaviour of rational approximations can be demonstrated by the following benchmark problem based on Kotanchek function (see for example Salazar Celis et al.), on the  $[0,4] \times [0,4]$  interval (Figure 2):

$$f(x, y) = \frac{e^{-(y-1)^2}}{1.2 + (x-2.5)^2} \quad (8)$$

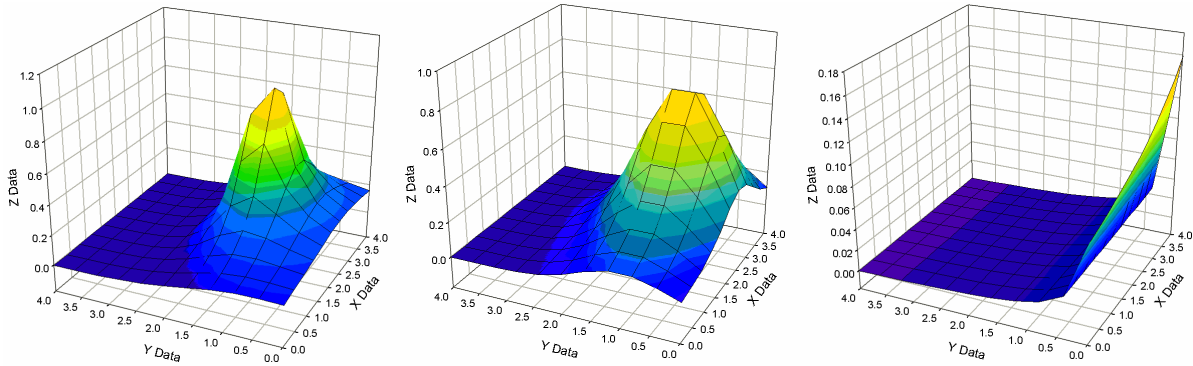


**Figure 2: Kotanchek function benchmark problem: exact function (left), second order approximation (centre), linear (right)**

It can be concluded that, although the linear form of the rational approximation describes the global behaviour rather poorly, such approximations can be useful in the mid-range approximation framework of MAM.

## Weight Coefficients

The weight coefficients influence the relative contribution of information on function values (and their derivatives, if available). Their choice strongly influences the difference in the quality of the approximations in different regions of the design variable space. Since the optimum point usually belongs to the boundary of the feasible region, the approximation functions should be more accurate in that region. Thus, the information at the points located near the boundary of the feasible region is to be treated with greater weights. This can be achieved by allocating an appropriate weight to the value of a constraint function at a point, e.g.  $w_{pj}^C = e^{-4|F_j(\mathbf{x}_p)-1|}$ .

In a similar manner a larger weight  $w_{pj}^O$  can be allocated to a design with a better objective function, see Toropov et al. (1995), van Keulen et al. (1996, 1997), van Keulen and Toropov (1997) for more details. Numerical examples showed, however, that the effect of this additional weight coefficient is relatively small.

The weight coefficients finally used for the weighted least squares fitting are now taken as  $w_{pj}^E = w_{pj}^C w_{pj}^O$ .

After a number of optimization steps have been carried out, a database with response function values becomes available. In addition to these design points available from the database, new designs are evaluated as part of a step

in the optimization process. In order to achieve good quality approximations in a current search sub-domain, a selection of plan points must be made. All designs located in the current search sub-domain will be included in the weighted least squares fitting (if the corresponding response function has been successfully evaluated, of course). Generally, points located far from the current search sub-domain would not contribute to the improvement of the quality of the resulting approximation functions in the current search sub-domain. For this reason only points located in the neighbourhood of the current search sub-domain are taken into account, as depicted in Figure 3. A box in the space of design variables, which is approximately 1.5 to 2.0 times larger than the box representing the current search domain, was found by numerical experimentation to be a reasonable choice for the size of the neighbourhood.

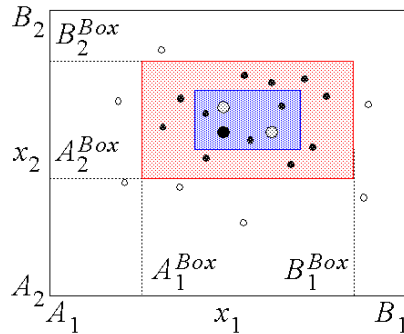


**Figure 3: Current search sub-domain and its neighbourhood (points marked ° are not included)**

### Plan of Experiments

Originally, a simple plan of experiments has been used (Toropov et al. 1993) which is based on  $N$  new points, where  $N$  is the number of design variables. The locations of these points were obtained by a perturbation of each design variable by a fraction of the corresponding size of the current search sub-domain. Generally, this scheme works well in conjunction with intrinsically linear approximations but, due to its simplicity, it may have some disadvantages. Firstly, it does not take into account design points which are already located in the present search sub-domain and, therefore, newly evaluated designs may be located too close to previously evaluated designs. Secondly, the scheme is inflexible with respect to the situation when the analysis crashed or did not converge (Toropov et al. 1999).

In the present work, new sampling points are generated randomly. Each added point is checked for calculability of the response function and, if the check fails, a new point is generated until a required number of plan points (all passing the check) are obtained. To improve the quality of the random plan, a constraint on the minimal distance between the points is imposed. Analytical tests have shown that this can improve the quality of the approximate functions and as a result reduce number of MAM iterations.

### Trust Region Strategy

After having solved the approximate optimization problem, a new trust region (search subregion in the design variable space) must be defined, i.e. its new size and its location have to be specified. This is done on the basis of a strategy summarized here.

The first step is to evaluate several indicators which are the basis for the strategy. The first indicator is the quality index of the approximation functions. It is defined as the largest relative approximation error at the set of design variables corresponding to the solution of the approximate optimization problem. The quality of the approximation functions is then categorized as "bad", "reasonable" or "good". The second indicator is the location of the sub-optimum point in the current trust region. When the obtained point does not belong to the boundary of the trust region, the solution is considered as "internal", otherwise it is denoted as "external". The third and fourth indicators are based on the movement history. For that purpose the angle between the last two move vectors is calculated. This will be the basis to identify the movement as "backward" or "forward". If the move vectors are nearly parallel, the convergence history will be labelled as "straight", otherwise it is marked as "curved". The fifth

indicator, used in the termination criterion, is the size of the present trust region. According to this indicator, the size can be "small" or "large". The sixth indicator is based on the value of the most active constraint. It is used to label the current solution as "close" or "far" from the boundary of the feasible and infeasible regions in the space of design variables. Once the indicators have been determined, the trust region is moved and resized. A summary of the move limit strategy as well as termination criteria is presented in Table 1.

If the obtained point does not pass the check for calculability of the response functions, the trust region is reduced and the approximated problem (2) is solved again. The only essential assumption here is that all functions of the optimization problem exist at the starting point.

Approximations "poor"					
"Small"		"Large"			
Stop: No convergence found		"Straight"		"Curved"	
		Reduce moderately or even enlarge		Reduce	
Approximation "reasonable"					
"Internal"			"External"		
"Small"	"Large"		"Backward"	"Forward"	
Stop: Convergence found	"Close"	"Far"	Reduce	"Straight"	"Curved"
	Reduce	Reduce		Enlarge	Keep size
Approximations "good"					
"Internal"			"Boundary"		
"Small"	"Large"		"Backward"	"Forward"	
Stop: Convergence found	"Close"	"Far"	Reduce	"Straight"	"Curved"
	Reduce	Reduce		Keep model & Enlarge	Keep model & Keep size

**Table 1: Overview of trust region strategy**

#### IV. Optimization Results

The results of the single point (100% speed) optimization are summarized in the pictures below. The solution was obtained after 14 iterations of MAM using 101 CFD analyses. It should be mentioned that for this run the algorithm used a "cheap" option to build approximate functions generating  $N+4$  sampling points ( $N=30$ ) in the 1<sup>st</sup> iteration and adding only 5 points in each next iteration.

The averaged efficiency was increased by 1.28% (from 0.856 to 0.867). It can be noticed that a radial distribution of the efficiency was improved between 8-17% and 40-75% span but dropped down between 30-40% and 75-90% span (see Fig. 4).

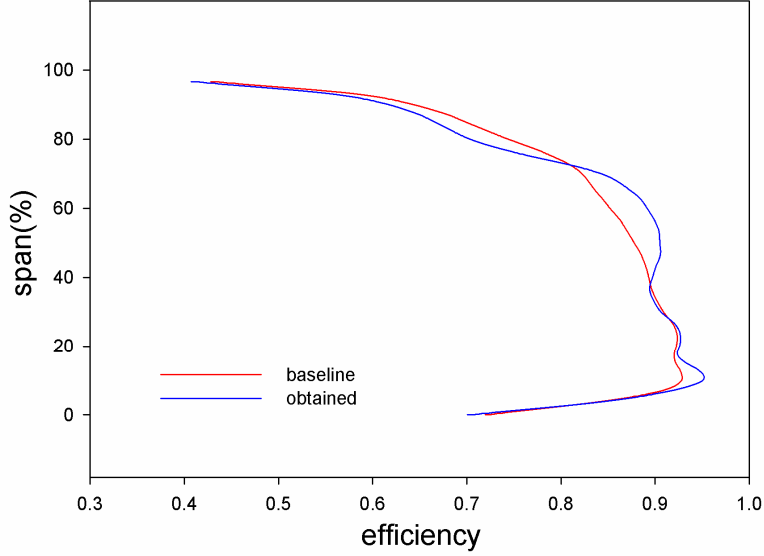


**Figure 4: Efficiency variations in radial direction for baseline (red) and obtained design (blue)**

In order to improve the efficiency profile, a second optimization run was performed using additional constraints imposed on the efficiency at 6 points along the radial direction:  $\eta_{optimal} \geq \eta_{baseline}$ . For this case, MAM generated  $N$  sampling points in each iteration. The optimization has achieved 1.9% efficiency increase after 11 iterations and 331 CFD analyses. As was expected, the optimal profile has been shifted in respect to the baseline curve toward increase over the full span range, Fig. 5. The initial and optimized blade shapes are compared in Fig. 6 using two-dimensional radial sections cut on 0% (hub), 20%, 40%, 60%, 80%, and 100% (tip) span.

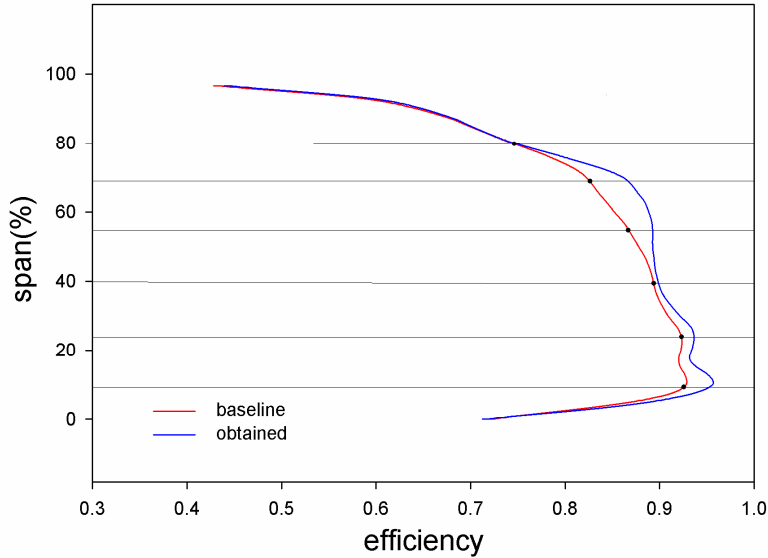


**Figure 5: Efficiency for baseline (red) and obtained design (blue) after the optimization with additional constraints on radial profile of the efficiency**

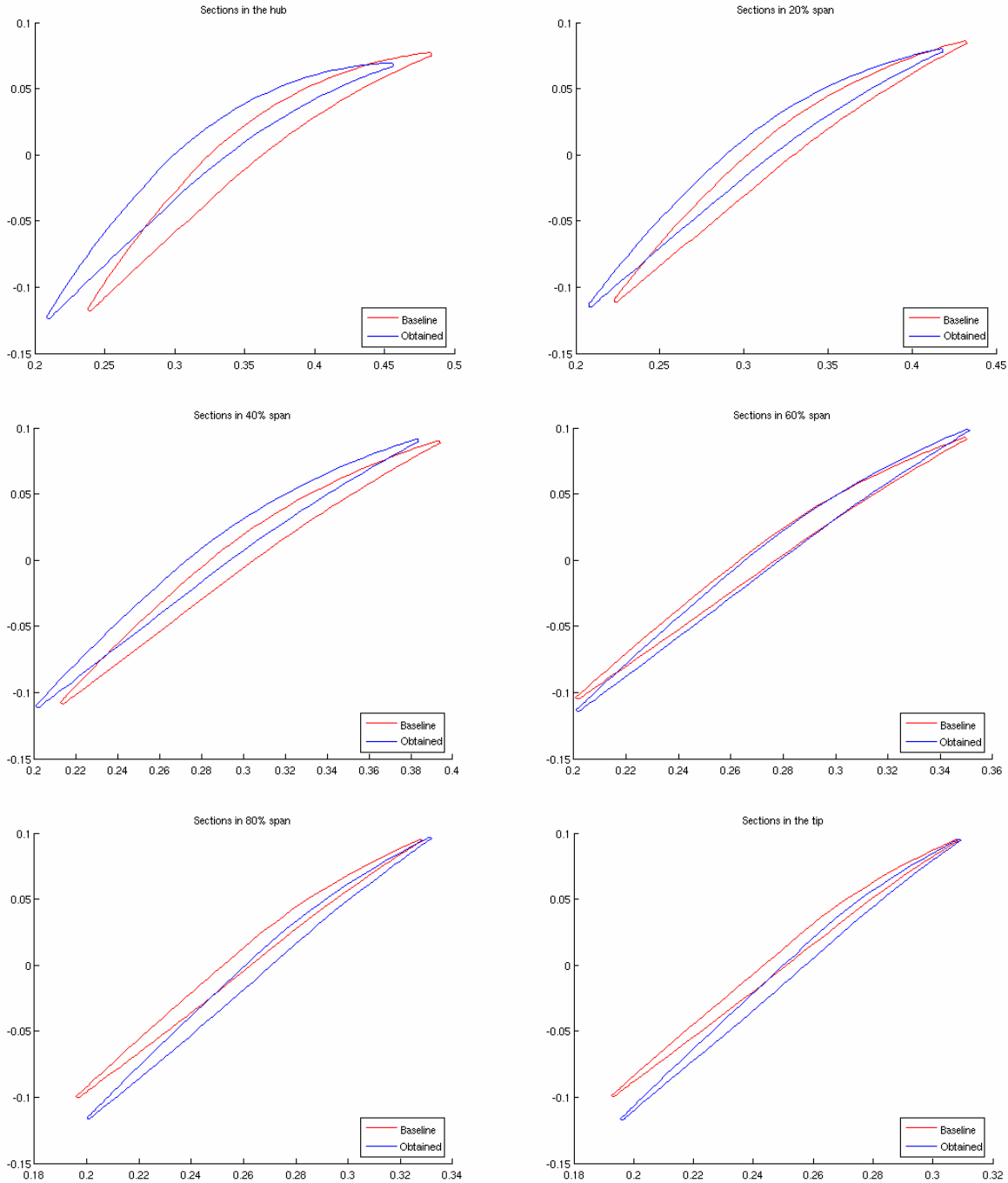


**Figure 6: Two-dimensional radial sections for baseline and obtained design**

It should be noted that in the above cases the multiplicative approximate functions were used. For comparison, a third case has been run based on rational functions. The optimization reached almost the same result after 6 MAM iterations. The quality of the approximations in each iteration has been categorizing as "good".

The obtained design has been checked for the off-design performance. It appeared that the entire characteristic was raised at a working point (100%) and also at 95% and 105% speed, Fig. 7.

Based on 30 processors (64 bit Opteron 2.4Hz) the above problem has been solved in 2 days. Work is now ongoing to solve the same problem on a larger scale with  $N > 100$ .

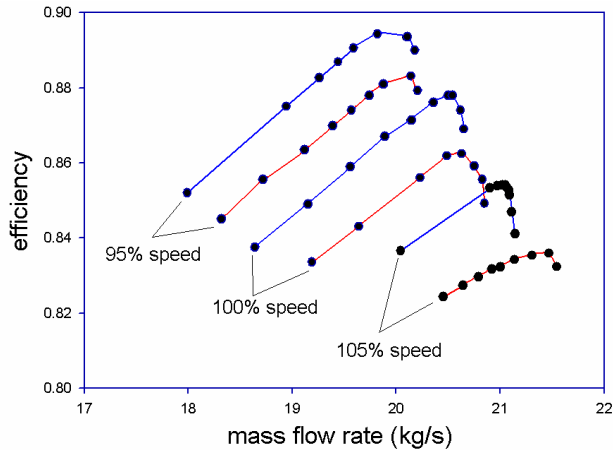


**Figure 7: Full characteristics for baseline (red) and obtained design (blue)**

## V. Acknowledgment

Authors are grateful for the financial support provided by the Department of Trade and Industry within the CFMS R&D programme.

## References

- Box, G.E.P., and Draper, N.R. (1987). Empirical model-building and response surfaces. New York: John Wiley and Sons.
- Burgee, S. L., Watson, L.T., Giunta, A.A., Grossman, B., Haftka, R.T. and Mason W.H. (1994). Parallel Multipoint Variable-Complexity Approximations for Multidisciplinary Optimization. Proceedings of the IEEE Scalable High-Performance Computing Conference, pp. 734-740, June 1994.
- Celis Salazar, O., Cuyt, A., and Verdonk, B. (2007). Rational approximation of vertical segments. Numerical algorithms, 45:375-388
- Lapworth L and Shahpar, S. (2004) Design of gas turbine engines using CFD, ECCOMAS 2004, July 24 – July 28, 2004.
- Shahpar, S. (2004). Automatic Aerodynamic Design Optimisation of Turbomachinery Components – An Industrial Perspective”, Invited Lecture at VKI, Belgium LS-2004-07.
- Shahpar S. and Lapworth B.L. (2003). PADRAM: Parametric Design and Rapid Meshing System for Turbomachinery Optimisation. Paper GT-2003-38698, ASME Turbo Expo, Atlanta Georgia, June 16-19, 2003.
- Toropov, V.V., Filatov, A.A., and Polynkin, A.A. (1993). Multiparameter structural optimization using FEM and multipoint explicit approximations. Structural Optimization 6:7-14.
- Toropov, V.V., Markine, V.L., and Holden, C.M.E. (1999). Use of mid-range approximations for optimization problems with functions of domain-dependent calculability, Proceedings of 3rd World Congress of Structural and Multidisciplinary Optimization, Buffalo, NY.
- van Keulen, F., Toropov, V.V., and Markine, V.L. (1996). Recent refinements in the multi-point approximation method in conjunction with adaptive mesh refinement. In McCarthy, J.M., ed., Proceedings of ASME Design Engineering Technical Conferences and Computers in Engineering Conference, Irvine, CA: 96-DETC/DAC-1451. 1-12.
- van Keulen, F., Polynkine, A.A., and Toropov, V.V. (1997). Shape optimization with adaptive mesh refinement: Target error selection strategies. Engineering Optimization 28:95-125.
- van Keulen, F., and Toropov, V.V. (1997). New developments in structural optimization using adaptive mesh refinement and multi-point approximations. Engineering Optimization 29:217-234.